An Algorithm for Calculating Transient Magnetic Field and Induced Voltage Inside Wind Turbine Tower Under Lightning Stroke

Zhang Xiaoqing and Zhang Yongzheng

School of Electrical Engineering
Beijing Jiaotong University, Beijing, 100044, China
zxqiong@hotmail.com, zhangyz2@126.com

Abstract ─ This paper proposes an efficient algorithm for predicting the transient magnetic field and induced voltage inside wind turbine tower under lightning stroke. The continuous tower body is simplified as a discrete multiconductor system consisting of longitudinal and transverse branches. On the basis of the lightning current responses in the multiconductor system, the analytic formulas of the transient magnetic field are derived from the vector potential. These formulas can take account of the impact of the wavefront steepness of lightning current on the transient magnetic field. A discretization scheme is further presented to calculate the magnetic flux passing through a conductor loop. The induced voltage can be determined by finding the time rate of change of the magnetic flux. The results obtained from the proposed algorithm are also compared with those from the software Ansoft and circuit method.

Index Terms ─ Induced voltage, lightning, magnetic field, transient analysis, wind turbine tower.

I. INTRODUCTION

With a rapid growth in the utilization of wind energy for electric power supply, wind turbines (WTs) have recently increased constantly in size and rated capacity. WTs are particularly susceptible to lightning stroke owing to their tall structure and exposed position. When a lightning strikes directly to a WT, a large lightning current flows through the body of the WT and generates the transient magnetic field inside its tower. There are a considerable number of conductor loops formed by power lines, signal cables and metal conduits in the bottom space of the tower. The transient magnetic field passes through these conductor loops and induces high voltages in them. It is well known that electronic equipment is very sensitive to the electromagnetic interference and has rather low insulation strength. Component failure and equipment damage may be caused by the transient magnetic field and induced voltage. From the point of view of lightning protection design of WTs, it is necessary to predict the transient

magnetic field and induced voltage inside the tower under lightning stroke. However, previous research mainly focused on the circuit analysis of the lightning transients of WTs. A few models were presented for predicting the lightning surge overvoltage and transient potential rise in WT systems [1-3]. There is almost no published literature on calculation of the transient magnetic field and induced voltage inside the tower. Although a set of empirical formulas have been given for estimation of the induced voltage amplitude [4-5], these formulas lack a high precision and fail to give the complete induced voltage waveform due to a deficiency in the exact analysis of the transient magnetic field. For an improvement on calculation of the transient magnetic field and induced voltage inside the tower, an efficient algorithm is proposed in this paper. In the proposed algorithm, the differential formulas of the transient magnetic field are first derived from the vector potential. A suitable discretization scheme is implemented to determine the magnetic flux passing through the conductor loop. Then, the induced voltage can be obtained by calculating the time rate of change of the magnetic flux. A numerical example has been given for examining the validity of the proposed algorithm, which shows that the proposed algorithm has the capability of quantitatively predicting the transient magnetic field and induced voltage inside the tower.

II. DISCRETIZATION DESCRIPTION OF WT TOWER

An actual WT tower is a tubular circular truncated cone, as shown in Fig. 1 (a). During a lightning stroke, the lightning current usually injects into the tower body from its top. For the purpose of electromagnetic transient analysis, the continuous conducting shell of the tower body may be divided into a discrete multiconductor system formed by longitudinal and transverse branches, as illustrated in Fig. 1 (b) [2-3, 6]. In the multiconductor system, each segmental arc of the transverse braches is replaced by its respective chord for simplification of the transient calculation. All the branches are taken as the

cylindrical conductors and the radii are estimated from their respective average cross-sections. Then, the multiconductor system is converted into an equivalent circuit consisting of resistances, inductances and capacitances. A current source representing the injected lightning current is applied to the top nodes of the equivalent circuit, whose parameters are taken from the technical specification of lightning protection [7]. The current distribution on all the branches can be determined by numerically solving the node voltage equations of the equivalent circuit. The detailed calculating procedure has been given in [2-3, 8-9] and will not been described here. On the basis of the current distribution, the transient magnetic field can be further calculated inside the tower.
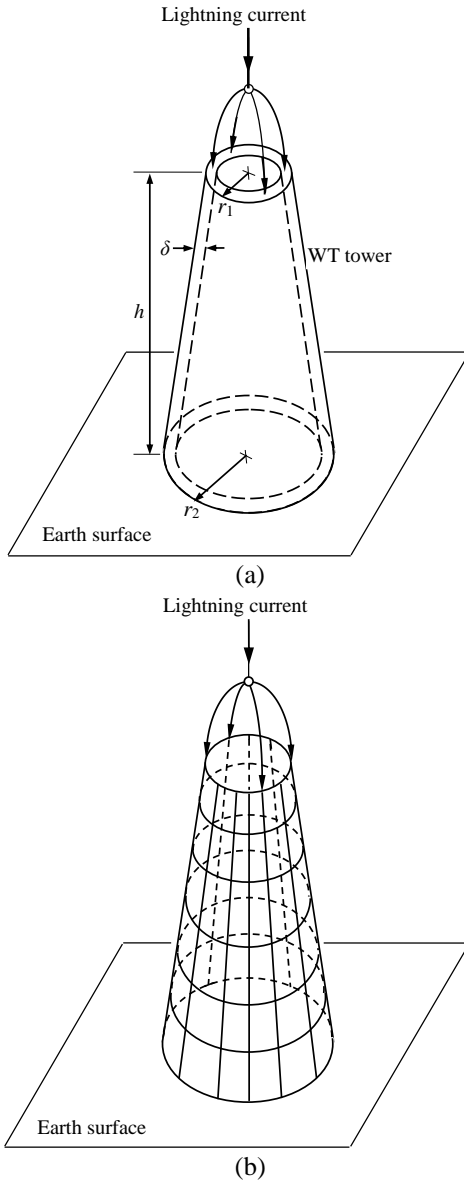
Fig. 1. (a) Tower body and (b) multiconductor system.

III. TRANSIENT MAGNETIC FIELD EQUATIONS

The transient electromagnetic fields in free space may be described by the time-dependent Maxwell equations. Considering the need of analyzing the magnetic induction effect, the solution of Maxwell equations is discussed only for magnetic field. The solution of magnetic field is based on the vector potential A:

$$B = \nabla \times A. \tag{1}$$

The general expression of the vector potential A is [10]:

$$A(r,t) = \frac{\mu_0}{4\pi} \int_\Omega \frac{J(r', t - \frac{R}{c})}{R} d\Omega, \tag{2}$$

where μ_0 is the permeability ($4\pi \times 10^{-7}$H/m), c is the speed of light, ε_0 is the permittivity [$(10^{-9}/36\pi)$ F/m] and J is the current density. The geometric factors associated with (2) are illustrated in Fig. 2. For a longitudinal branch in the multiconductor system, as shown in Fig. 3, consider a differential current-carrying segment dl. In cylindrical coordinates, the differential current element $J(r', t-R/c)d\Omega$ becomes $i(r', \alpha, z', t-R/c)dl$ and the resulting differential vector potential is found by [11-13]:

$$dA = \frac{\mu_0}{4\pi} \frac{1}{R} i(r', \alpha, z', t - R/c)dl. \tag{3}$$

Substituting $dl = dl\cos\gamma \mathbf{r} + dl\sin\gamma \mathbf{k}$ into (3) yields:

$$dA_\theta = 0$$
$$dA_r = \frac{\mu_0 dl \cos\gamma}{4\pi} \frac{1}{R} i(r', \alpha, z', t - R/c)\mathbf{r}$$
$$dA_z = \frac{\mu_0 dl \sin\gamma}{4\pi} \frac{1}{R} i(r', \alpha, z', t - R/c)\mathbf{k}. \tag{4}$$

In terms of (1) and (4), the differential magnetic flux density due to dl can be derived from the differential vector potential dA:

$$dB = \nabla \times (dA) = \frac{1}{r} \frac{\partial(dA_z)}{\partial\theta} \mathbf{r} - \left[\frac{\partial(dA_z)}{\partial r} - \frac{\partial(dA_r)}{\partial z} \right] \boldsymbol{\theta} - \frac{1}{r} \frac{\partial(dA_r)}{\partial\theta} \mathbf{k}. \tag{5}$$
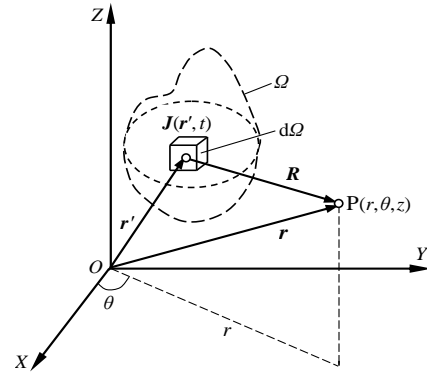
Fig. 2. Geometry for general expression of vector potential.
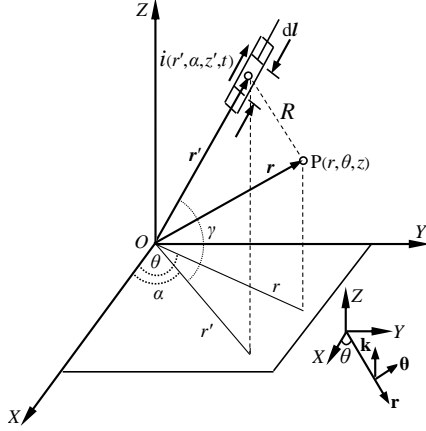
Fig. 3. A longitudinal branch.

In Fig. 3, R may be expressed by:

$$R = \sqrt{r^2 + r'^2 - 2rr'\cos(\theta - \alpha) + (z - z')^2}. \quad (6)$$

Letting $\xi = t - R/c$ and $\Phi = \theta - \alpha$, the derivatives of $i(r', \alpha, z', t - R/c)$ with respect to r, θ, z and t are written by:

$$\frac{\partial}{\partial r}[i(r', \alpha, z', t - R/c)] = -\frac{r - r'\cos\Phi}{cR}$$
$$\cdot \frac{\partial i(r', \alpha, z', \xi)}{\partial \xi}$$

$$\frac{\partial}{\partial \theta}[i(r', \alpha, z', t - R/c)] = -\frac{rr'\sin\Phi}{cR}$$
$$\cdot \frac{\partial i(r', \alpha, z', \xi)}{\partial \xi} \quad (7)$$

$$\frac{\partial}{\partial z}[i(r', \alpha, z', t - R/c)] = -\frac{(z - z')}{cR}$$
$$\cdot \frac{\partial i(r', \alpha, z', \xi)}{\partial \xi}$$

$$\frac{\partial}{\partial t}[i(r', \alpha, z', t - R/c)] = \frac{\partial i(r', \alpha, z', \xi)}{\partial \xi}.$$

This follows that:

$$\frac{\partial}{\partial r}[i(r', \alpha, z', t - R/c)] = -\frac{r - r'\cos\Phi}{cR}$$
$$\cdot \frac{\partial i(r', \alpha, z', t - R/c)}{\partial t}$$

$$\frac{\partial}{\partial \theta}[i(r', \alpha, z', t - R/c)] = -\frac{rr'\sin\Phi}{cR}$$
$$\cdot \frac{\partial i(r', \alpha, z', t - R/c)}{\partial t} \quad (8)$$

$$\frac{\partial}{\partial z}[i(r', \alpha, z', t - R/c)] = -\frac{z - z'}{cR}$$
$$\cdot \frac{\partial i(r', \alpha, z', t - R/c)}{\partial t}.$$

The following derivatives can be given from (6):

$$\frac{\partial}{\partial r}\left(\frac{1}{R}\right) = -\frac{r - r'\cos\Phi}{R^3}$$

$$\frac{\partial}{\partial \theta}\left(\frac{1}{R}\right) = -\frac{rr'\sin\Phi}{R^3} \quad (9)$$

$$\frac{\partial}{\partial z}\left(\frac{1}{R}\right) = -\frac{z - z'}{R^3}.$$

Substituting (4), (8) and (9) into (5) leads to the differential magnetic flux density:

$$dB_l = -\frac{\mu_0 dl \sin\gamma}{4\pi}\left[\frac{r'\sin\Phi}{R^3}i(r', \alpha, z', t - R/c)\right.$$
$$\left.+\frac{r'\sin\Phi}{cR^2}\frac{\partial i(r', \alpha, z', t - R/c)}{\partial t}\right]\mathbf{r}$$
$$+\frac{\mu_0 dl \sin\gamma}{4\pi}\left[\frac{r - r'\cos\Phi}{R^3}i(r', \alpha, z', t - R/c)\right.$$
$$+\frac{z - z'}{cR^2}\frac{\partial i(r', \alpha, z', t - R/c)}{\partial t}$$
$$-\frac{\cot\gamma(z - z')}{R^3}i(r', \alpha, z', t - R/c) \quad (10)$$
$$\left.-\frac{\cot\gamma(z - z')}{cR^2}\frac{\partial i(r', \alpha, z', t - R/c)}{\partial t}\right]\boldsymbol{\theta}$$
$$+\frac{\mu_0 dl \cos\gamma}{4\pi}\left[\frac{r'\sin\Phi}{R^3}i(r', \alpha, z', t - R/c)\right.$$
$$\left.+\frac{r'\sin\Phi}{cR^2}\frac{\partial i(r', \alpha, z', t - R/c)}{\partial t}\right]\mathbf{k}.$$

In a similar manner, the transient magnetic field equation can be derived for a transverse branch in the multiconductor system. As shown in Fig. 4, the differential magnetic flux density is given by:

$$dB_t = \frac{\mu_0 dl \sin\varphi}{4\pi}\left[\frac{z - z'}{R^3}i(r', \alpha, z', t - R/c)\right.$$
$$\left.+\frac{z - z'}{cR^2}\frac{\partial i(r', \alpha, z', t - R/c)}{\partial t}\right]\mathbf{r}$$
$$-\frac{\mu_0 dl \cos\varphi}{4\pi}\left[\frac{z - z'}{R^3}i(r', \alpha, z', t - R/c)\right.$$
$$\left.+\frac{z - z'}{cR^2}\frac{\partial i(r', \alpha, z', t - R/c)}{\partial t}\right]\boldsymbol{\theta}$$
$$+\frac{\mu_0 dl \sin\varphi}{4\pi}\left[\frac{R^2 - r^2 + rr'\cos\Phi}{R^3 r}\right. \quad (11)$$
$$\cdot i(r', \alpha, z', t - R/c) - \frac{r - r'\cos\Phi}{cR^2}$$
$$\cdot \frac{\partial i(r', \alpha, z', t - R/c)}{\partial t}$$
$$+\frac{\cot\varphi \, r'\sin\Phi}{R^3}i(r', \alpha, z', t - R/c)$$
$$\left.+\frac{\cot\varphi \, r'\sin\Phi}{cR^2}\frac{\partial i(r', \alpha, z', t - R/c)}{\partial t}\right]\mathbf{k}.$$

On the right-hand sides of (10) and (11), the terms including the current are the induction field and are the radiation field [14]. The radiation field can reflect the impact of the wavefront steepness of lightning current on the transient magnetic field. In addition, the presence of the ground is taken into account by the image method [10,13]. The image branches are installed below the earth surface. From the point of view of engineering application, the real and the image branches are considered to be symmetrical about the earth surface [10,15]. Each branch, whether it is the real or the image, needs to be subdivided into a sufficient number of segments [16]. The length of each segment is so short that the current distribution on it is approximately uniform. Then, (10) or (11) is used to calculate its magnetic field component. The magnetic flux density at an arbitrary spatial point inside the tower can be found by vectorially summing the magnetic field components contributed from the short segments on all the real and the image branches.
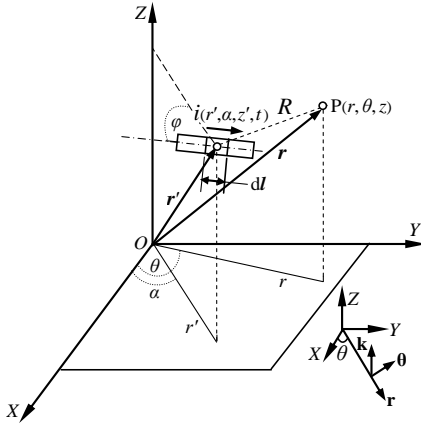
Fig. 4. A transverse branch.

IV. CALCULATION OF INDUCED VOLTAGE

A spatial conductor loop is shown in Fig. 5. The magnetic flux passing through the loop can be expressed by the surface integral of the magnetic flux density:

$$\Psi(t) = \int_S \boldsymbol{B} \cdot \mathrm{d}\boldsymbol{S}. \tag{12}$$

From Faraday's law of electromagnetic induction, the induced voltage in the loop is calculated by the time rate of change of the magnetic flux:

those including the first derivative of the current

$$u(t) = \frac{d\Psi(t)}{dt}. \tag{13}$$

Since the magnetic field distribution on the surface of the loop is usually non-uniform, the surface needs to be subdivided into a series of subareas. On each subarea, the magnetic flux density is considered to be uniform.

With such a discrete approximation to (13), the magnetic flux is calculated by:

$$\Psi(j\Delta t) \approx \sum_{k=1}^{N} B_k(j\Delta t)\Delta S_k \cos\theta_k \quad (j=1,2\cdots,J_{\mathrm{m}}), \tag{14}$$

where Δt is the time step, N is the total number of the subareas and J_{m} is the maximum number of the time steps. In terms of (13) and (14), the induced voltage can be determined by:

$$u(j\Delta t) = \frac{\Psi(j\Delta t) - \Psi((j-1)\Delta t)}{\Delta t} \quad (j=1,2\cdots,J_{\mathrm{m}}). \tag{15}$$
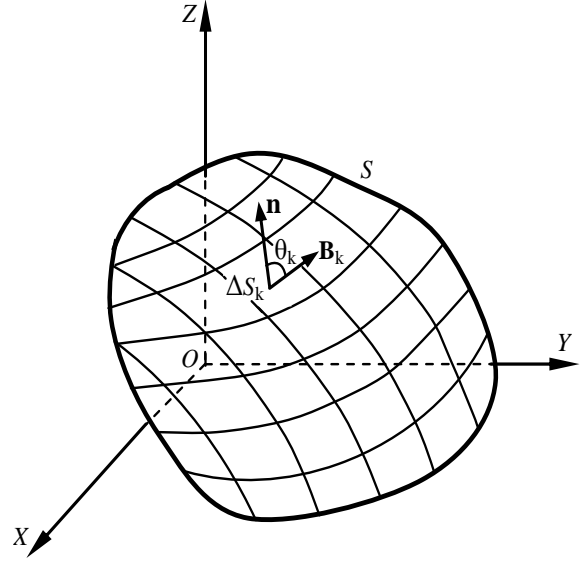
Fig. 5. Subdivision of the loop surface.

V. NUMERICAL EXAMPLE

A. Magnetic field

A Chinese-built WT with rated power of 2MW is considered here. The dimensions of its tower are $r_1 = 1.32$ m, $r_2 = 2.1$ m, $h = 81.5$ m and $\delta = 0.024$ m, as shown in Fig. 6 (a). The parameters of the injected lightning current are 10/350 μs and 100 kA [7]. The amplitude distributions of the magnetic flux density are calculated for two cross-sections locating at $z = 80$ m and $z = 40$ m, as shown in Figs. 6 (b)-(c). Due to the spatial distribution symmetry, only a quarter of each distribution surface is depicted here. For the spatial points on the plumb line bounded by (1.3 m, π/4, 40 m) and (1.3 m, π/4, 80 m), the magnetic flux density amplitudes are also given in Fig. 6 (d), which are calculated by the proposed algorithm and software Maxwell 3D of Ansoft [6,17], respectively. The Ansoft calculation is based on the finite-element method (FEM). It can be seen from Figs. 6 (b)-(c) that, the magnetic flux density becomes higher near the tower wall and reaches a maximum under the point where the lightning current is injected. By contrast, the magnetic field is rather weak in the central zone.

(a)

(d)
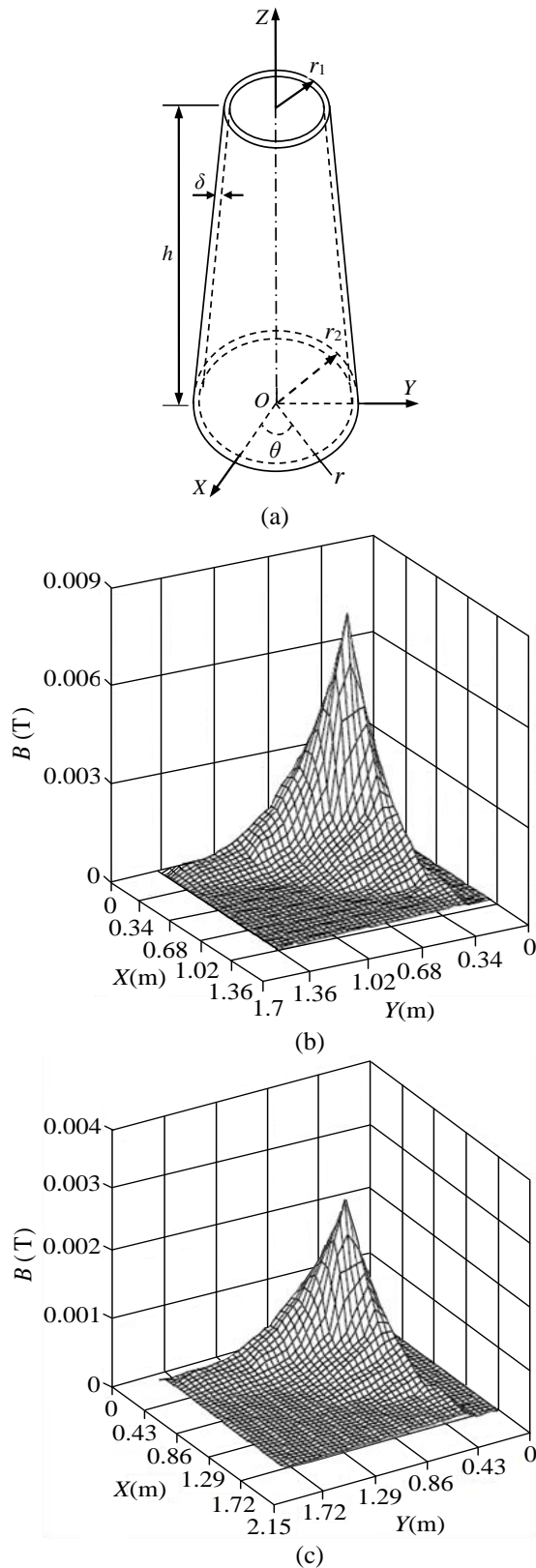
Fig. 6. (a) Dimension of the tower; (b) amplitude distribution of magnetic flux density at z = 80 m; (c) amplitude distribution of magnetic flux density at $z=40$ m; (d) magnetic flux density amplitudes on the plumb line.

B. Induced voltage

The dimensions of the tower and lightning current parameters are the same as above. A square conductor loop with 0.3 m × 0.3 m is located on the plane YOZ, as illustrated in Fig. 7 (a). The geometric center of the loop is positioned on a line with two endpoints A and B. The coordinates of A and B are (1.0 m, $\pi/2$, 10 m) and (1.0 m, $\pi/2$, 0.16 m). Figures 7 (b) and (c) show the induced voltage waveforms at geometric centers A and B, respectively. Figure 7 (d) gives the induced voltage amplitudes at the distinct geometric centers along the line AB, where the corresponding results calculated by the circuit method are given simultaneously for comparison. In the circuit method, each side of the loop is represented by a π-type circuit consisting of resistance, inductance and capacitance. The induction effect is simulated by the mutual inductances and coupling capacitances between the sides of the loop and branches of the multiconductor system of the tower [18]. The corresponding simulation procedure has been stated in [18-19]. Figure 7 signifies that the induced voltage levels are high and can cause serious damage to the electronic equipment involved in these loops during a lightning stroke.

In Fig. 6 (d) and Fig. 7 (d), comparison of the results obtained from the proposed algorithm with those from the software Ansoft and circuit method shows that a better agreement appears between them. To a large extent, this confirms the validity of the proposed algorithm.

(b)

(c)

(a)

(b)

(c)

(d)
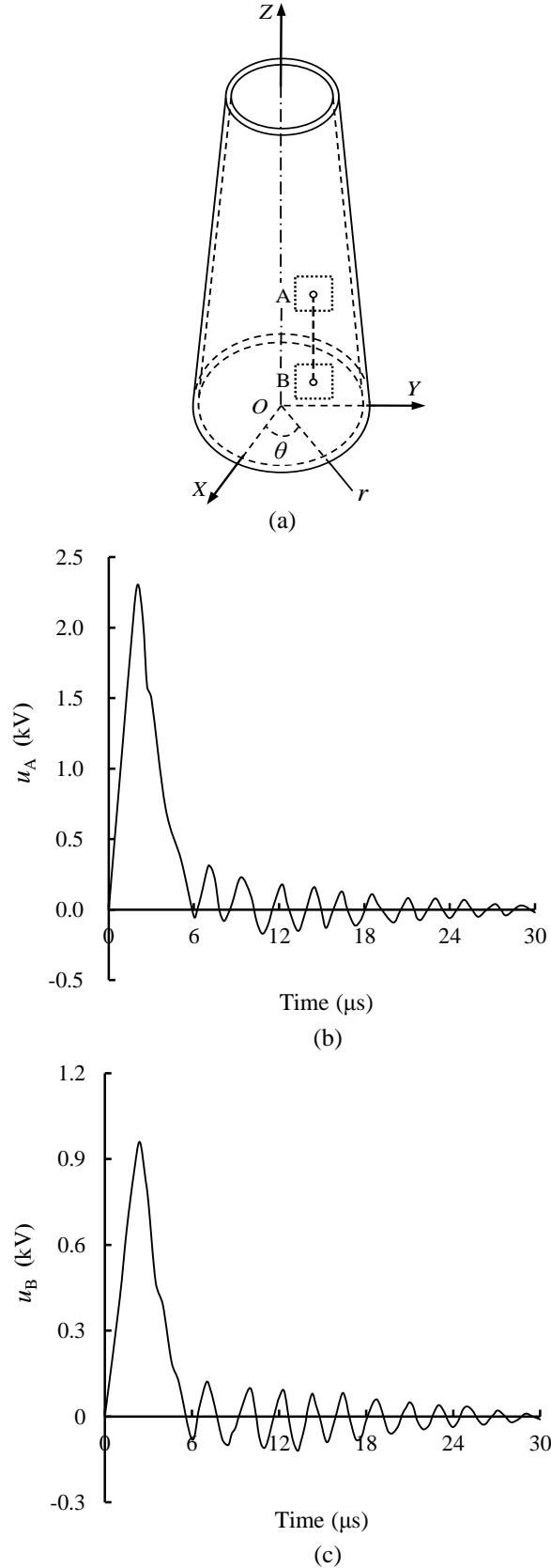
Fig. 7. (a) Conductor loop inside the tower; (b) induced voltage waveform in geometric center A; (c) induced voltage waveform in geometric center B; (d) amplitude distribution of induced voltage on line AB.

VI. CONCLUSION

An efficient algorithm has been proposed for predicting the transient magnetic field and induced voltage inside the WT tower under lightning stroke. The proposed algorithm simplifies the large-sized continuous tower body into a discrete multiconductor system. Based on the vector potential, analytic formulas have been presented for calculating the transient magnetic field generated by longitudinal and transverse current-carrying branches in the multiconductor system. The magnetic flux passing through a conductor loop is determined by evaluating the surface integral of the transient magnetic field over the surface of the conductor loop in a discretization manner. The induced voltage in the conductor loop can be obtained by finding the time rate of change of the magnetic flux. A numerical example has been given for an actual WT tower and the validity of the proposed algorithm has been checked by comparing the results obtained from the proposed algorithm with those from the software Ansoft and circuit method. The proposed algorithm is useful in quantitative prediction of the transient magnetic field and induced voltage inside the large-sized WT tower and can provide a basis for lightning protection design of multi-megawatt WTs.

ACKNOWLEDGMENT

REFERENCES

[1] D. Romero, J. Montanyà, and A. Candela,

"Behavior of the wind-turbines under lightning strikes including nonlinear grounding system," *International Conference on Renewable Energy and Power Quality*, Barcelona, Spain, pp. 1-6, 1-2 Apr. 1-2, 2004.

[2] X. Q. Zhang, Y. Z. Zhang, and C. H. Liu, "A complete model of wind turbines for lightning transient analysis," *Journal of Renewable and Sustainable Energy*, vol. 6, 013113, 2014.

[3] X. Q. Zhang, "Lightning transient simulation of wind turbine towers," *International Review of Electrical Engineering*, vol. 7, no. 1, pp. 3505-3511, 2012.

[4] IEC 62305-4: 2006, IDT, *Protection against Lightning—Part 4: Electrical and Electronic Systems within Structures*, IEC Geneva, Switzerland, 2006.

[5] P. Hasse, *Overvoltage Protection of Low Voltage Systems*, The Institution of Engineering and Technology, London, UK, 2008.

[6] C. Buccella and A. Orlandi, "An efficient technique for the evaluation of lightning-induced voltage in a cylindrical vessel containing charged oil," *IEEE Trans. Industry Applications*, vol. 39, no. 2, pp. 368-373, 2003.

[7] National Standard, GB 50057-2010, *Design Code for Protection of Structures Against Lightning*, Chinese Plan Press, Beijing, China, 2010.

[8] L. Sluis, *Transients in Power Systems*, John Wiley & Sons Ltd., 2002

[9] X. Q. Zhang, "Calculation of lightning transient responses on wind turbine towers," *Mathematical Problems in Engineering*, vol. 2013, Article ID 757656, pp. 1-9, 2013

[10] C. Z. Feng, *Electromagnetic Field Theory*, Higher Education Press, Beijing, China, 2002.

[11] G. Guarnieri, S. Selleri, G. Pelosi, C. Dedeban, and C. Pichot, "Innovative basis and weight functions for wire junctions in time domain moment method," *IEE Proceedings Microwaves, Antennas and Propagation*, vol. 153, no. 1, pp. 61-66, 2006.

[12] Z. X. Zhou and J. S. Tyo, "An adaptive time-domain integral equation method for transient analysis of wire scatterer," *IEEE Trans. Antennas and Wireless Propagation Letters*, vol. 49, no. 8,

pp. 1123-1129, 2001.

[13] B. S. Gru and H. R. Hiziroğlu, *Electromagnetic Field Theory Fundamentals*, Cambridge University Press, Cambridge, UK, 2004.

[14] F. Rachidi, W. Janischewskyj, A. M. Hussein, C. A. Nucci, S. Guerrieri, B. Kordi, and J. S. Chang, "Current and electromagnetic field associated with lightning-return strokes to tall towers," *IEEE Trans. Electromagnetic Compatibility*, vol. 43, no. 3, pp. 356-367, 2001.

[15] D. Pavanello, F. Rachidi, M. Rubinstein, J. L. Bermudez, and C. A. Nucci, "On the calculation of electromagnetic fields radiated by lightning to tall structures," 27th *International Conference on Lightning Protection*, Avignon, France, pp. 1-8, Sep. 13-16, 2004.

[16] A. R. Bretones, R. G. Martin, and A. Salinas, "Dotig1, a time-domain numerical code for the study of the interaction of electromagnetic pulses with thin-wire structures," *Compel-The International Journal for Computation and Mathematics in Electrical and Electronic Engineering*, vol. 8, no. 1, pp. 39-61, 1989.

[17] Ansoft User's Guide–Maxwell 3D, 2006

[18] S. Cristina and A. Orlandi, "Calculation of the induced effects due to a lightning stroke," *IEE Proceedings-B*, vol. 139, no. 4, pp. 374-380, 1992.

[19] U. Y. Iosseli, A. S. Kothanov, and M. G. Stlyrski, *Calculation of Capacitances*, Electric Power Press, Moscow, Russia, 1987.

Zhang Xiaoqing received the M.Sc. and Ph.D. degrees from Tsinghua University, Beijing, China, in 1985 and 1990, respectively, both in High Voltage Engineering. Since 1993, he has been in the School of Electrical Engineering, Beijing Jiaotong University, where he is currently a Senior Research Fellow. His research interests include electromagnetic transient simulation, lightning protection and high voltage insulation.